Pressure-induced metallization and resonant Raman scattering in Zn 1 x Mn x Te

Y. C. Lin, W. C. Fan, C. H. Chiu, F. K. Ke, S. L. Yang, D. S. Chuu, M. C. Lee, W. K. Chen, W. H. Chang, W. C. Chou, J. S. Hsu, and J. L. Shen

Citation: Journal of Applied Physics **104**, 013503 (2008); doi: 10.1063/1.2949707
View online: http://dx.doi.org/10.1063/1.2949707
View Table of Contents: http://scitation.aip.org/content/aip/journal/jap/104/1?ver=pdfcov
Published by the AIP Publishing

Pressure-induced metallization and resonant Raman scattering in $Zn_{1-x}Mn_xTe$

Y. C. Lin,[1] W. C. Fan,[1] C. H. Chiu,[1] F. K. Ke,[1] S. L. Yang,[1] D. S. Chuu,[1] M. C. Lee,[1] W. K. Chen,[1] W. H. Chang,[1] W. C. Chou,[1,a)] J. S. Hsu,[2] and J. L. Shen[2]
[1]*Department of Electrophysics, National Chiao Tung University, Hsinchu 30010, Taiwan, Republic of China*
[2]*Department of Physics, Chung Yuan Christian University, Chung-Li 32023, Taiwan, Republic of China*

(Received 5 March 2008; accepted 24 April 2008; published online 1 July 2008)

Pressure-induced resonant Raman scattering is adopted to analyze the zone-center optical phonon modes and crystal characteristics of $Zn_{1-x}Mn_xTe$ ($0 \leqq x \leqq 0.26$) thin films. The pressure (Pt) at which the semiconducting undergoes a transition to the metallic phase declines as a function of Mn concentration (x) according to the formula $Pt(x)=15.7-25.4x+19.0x^2$ (GPa). Pressure-dependent longitudinal and transverse optical phonon frequencies and the calculated mode Grüneisen parameters were adopted to investigate the influence of Mn^{2+} ions on the iconicity. The experimental results indicate that the manganese ions tend to increase the iconicity of ZnTe under ambient conditions, whereas an external hydrostatic pressure tends to reduce the iconicity and the bond length of $Zn_{1-x}Mn_xTe$. © *2008 American Institute of Physics*. [DOI: 10.1063/1.2949707]

I. INTRODUCTION

Dilute magnetic semiconductor (DMS) $Zn_{1-x}Mn_xTe$, in which a fraction of Zn element is replaced by Mn atoms, crystallizes in the zincblende (ZB) structure for $x \leqq 0.8$ under ambient conditions.[1] The magnetic properties of $Zn_{1-x}Mn_xTe$-related materials are currently a focus of research activities in numerous interesting investigations.[2–6] Magnetic ordering in semiconductors can arise from the superexchange interaction or free-carrier-mediated exchange interaction between magnetic ions. Long-range ferromagnetic orderings, mediated by holes, were observed in $Ga_{1-x}Mn_xAs$ (Ref. 7) and $In_{1-x}Mn_xAs$,[8] in which manganese ions act as acceptors. Alternatively, p-doped $Zn_{1-x}Mn_xTe$, in which magnetic ions are not dopants, exhibits ferromagnetism that is induced by the exchange interaction of free holes with the localized spins of Mn^{2+} ions.[3–6] Moreover, our recent high pressure study of n-doped ZnSe:Cl demonstrated that the hydrostatic pressure tends to reduce the carrier concentration, and that doping influences the metallic phase transition.[9] Therefore, the effect of applied pressure on the physical properties of DMS $Zn_{1-x}Mn_xTe$ will be of interest in future studies of the pressure-dependent magnetic properties of this material.

Pressure-induced phase transitions of ZnTe bulk crystal have been widely studied.[10–13] So far, all of the evidence has shown that the application of pressure to a semiconducting ZnTe exhibits a unique transition sequence. As the pressure is increased, the semiconducting ZB ZnTe phase (ZnTe I) first transforms to the other semiconducting cinnabar phase (ZnTe II), and then undergoes a transition to a metallic orthorhombic (*Cmcm*) phase (ZnTe III). These high-pressure phase behaviors differ from those of most II-VI semiconductors,[14–16] which transform from ZB (or wurtzite) first to the cinnabar structure and then to the rock-salt (NaCl) structure as external pressure is applied. Even though the NaCl phase is unstable and has not been observed in ZnTe at room temperature under any pressure, it has been revealed to be stable only at high temperature.[17] This result is attributed to the fact that ZnTe is the lowest ionic semiconductor in the II-VI family.[18] The transition pressure from nonmetallic ZnTe to metallic ZnTe III (*Cmcm*) phase is controversial. Optical-absorption measurements yield a transition pressure of 11.9 GPa.[10] The electrical resistance approach yields a transformation of 13–15 GPa.[11] The metallic phase of ZnTe, as revealed by Raman scattering, forms at above 14.2 GPa.[12] Moreover, the crystalline structure of the ZnTe phase III is determined to be 16 GPa using angle-dispersive powder-diffraction techniques with synchrotron radiation.[13] To resolve these unusual and controversial phase transitions at high pressure, Raman scattering under high pressure was performed to investigate ZnTe and $Zn_{1-x}Mn_xTe$ thin films up to 17.0 GPa. Furthermore, resonant Raman scattering (RRS) was adopted to enhance the Raman signal to identify more clearly the semiconductor-to-metal phase transition pressure. The crystalline stability, iconicity, and Grüneisen parameters (γ_i) of $Zn_{1-x}Mn_xTe$ ($0 \leqq x \leqq 0.26$) thin films were also studied.

II. EXPERIMENT

$Zn_{1-x}Mn_xTe$ samples with various Mn contents ($0 \leqq x \leqq 0.26$) were deposited at 300 °C by molecular beam epitaxy on (001) oriented semi-insulating GaAs substrates. The samples' thicknesses were fixed at about 0.7 μm, and the Mn composition was determined by energy-dispersive x-ray analysis. Raman spectra under ambient pressure were all recorded at 300 K and excited using the 514.5 nm line of an Ar^+ laser, while the 488.0 nm line from the Ar^+ laser was used in high-pressure experiments. High-pressure Raman measurements were all made at room temperature using a

a)Author to whom correspondence should be addressed. Electronic mail: wuchingchou@mail.nctu.edu.tw.

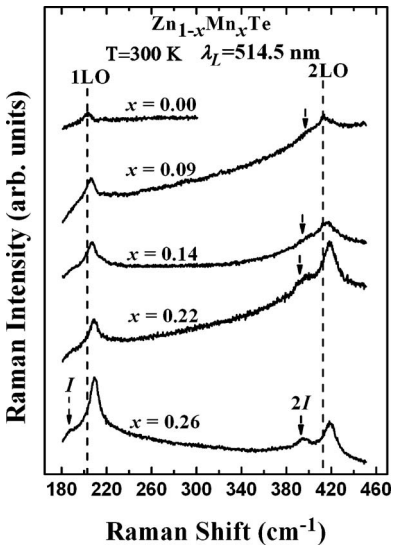

FIG. 1. Raman spectra of $Zn_{1-x}Mn_xTe$ ($0 \leqq x \leqq 0.26$) at 300 K under ambient pressure. The excitation source is a 514.5 nm line from an Ar^+ laser.

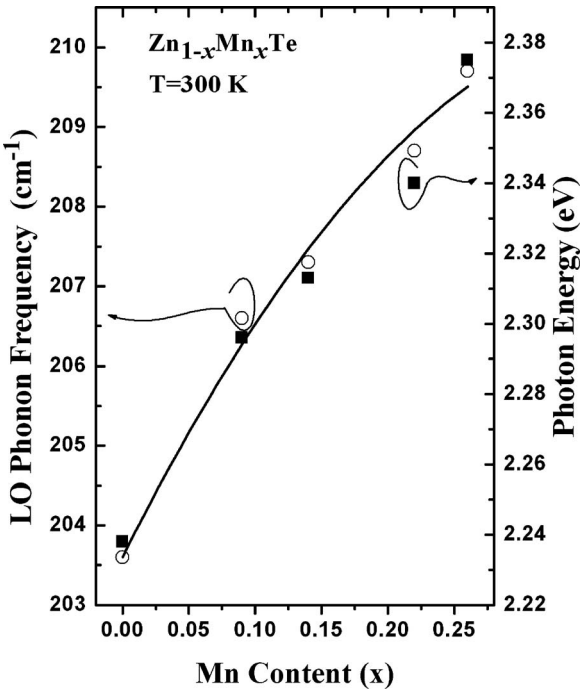

FIG. 2. Dependence of LO phonon frequencies (open circle) and PL energy (solid square) on Mn concentration (x) at room temperature. The solid curve is a quadratic polynomial fit for the LO phonon.

ruby-calibrated diamond anvil cell (DAC).[9] A liquid methanol-ethanol 4:1 mixture was utilized as the pressure-transmitting medium, and the pressure gradient was less than 0.2 GPa throughout the sample chamber. Before loading the $Zn_{1-x}Mn_xTe$ crystal into the DAC, the GaAs substrate was removed by mechanical polishing and chemical etching. Spectra were all obtained in backscattering configuration and analyzed by a SPEX 1404 double grating spectrometer equipped with a multichannel LN_2-cooled charge coupled device. The high-pressure experiments are reproducible for each specimen. The photoluminescence (PL) energies were obtained at 300 K, using the 488.0 nm line of an Ar^+ laser.

III. RESULTS AND DISCUSSION

Figure 1 presents the zone-center Raman spectra of $Zn_{1-x}Mn_xTe$ (x=0.00, 0.09, 0.14, 0.22, and 0.26), measured at room temperature and ambient pressure under $z(x+y,x+y)\bar{z}$ backscattering geometry. In this configuration, transverse optical (TO) phonons are forbidden and longitudinal optical (LO) phonons are allowed. As the Mn content increases, the 1LO and its overtone (2LO) phonon frequencies increase. Figure 2 plots the dependence of the 1LO phonon frequency and the PL energy on the Mn concentration (x). The increase in the LO phonon frequency with Mn content is due to the difference between atomic masses, $m_{Mn}(55) < m_{Zn}(65)$. As the Mn concentration increases, the PL energy is blueshifted and slowly approaches the incident laser energy. When the energy of the electronic transition energy is sufficiently close to the incident laser energy, the RRS effect occurs, enhancing the intensity of LO phonons. Based on the RRS condition,

$$h\nu_{\text{laser}} - mh\nu_{\text{LO}}(x,p) \approx E_{\text{exc}}(x,p), \tag{1}$$

where $h\nu_{\text{laser}}$ is the photon energy of the incident laser. $E_{\text{exc}}(x,p)$ and $h\nu_{\text{LO}}(x,p)$ are the electronic transition energy and the LO phonon energy, respectively, as functions of Mn content (x) and applied pressure (p). The m denotes the overtone order of LO phonons. Under ambient conditions, when the laser is fixed at 2.41 eV, the Raman scattering of the larger overtone phonon comes into resonance first (Fig. 1). As shown in Fig. 1, besides the LO mode, an impurity (I) mode and its overtone ($2I$) at the lower-frequency side of the LO phonon in $Zn_{1-x}Mn_xTe$ ($x>0$) are also visible. As the Mn content increases, the impurity (I and $2I$) modes shift to lower frequencies and become intense. Similar phenomena are also found in $Zn_{1-x}Mn_xSe$ (Ref. 15) and $Zn_{1-x}Cd_xSe$ (Ref. 16) II-VI ternary compounds. Since the impurity mode discussed herein lies between the LO and TO modes and can also be apparently observed at high pressures, it can be identified as the impurity mode of Mn in ZnTe. Accordingly, the zone-center optical phonon mode of $Zn_{1-x}Mn_xTe$ can be concluded to exhibit mixed mode behavior. This finding is consistent with an earlier work.[1]

Figure 3 shows the up-stroke pressure-dependent Raman spectra of the ZnTe thin film at up to 17.0 GPa. The TO mode, which is not allowed under ambient conditions before pressurization, appears at high pressures. The emergence of the TO mode can be attributed to the pressure-induced RRS enhancement and the deviation of the sample chip from the perfect backscattering geometry in the DAC. The LO and TO phonons both shift to higher frequencies with increasing pressure, wherein the shift is accompanied by clear changes in their intensities. The reduction in the lattice constant and the crystal volume under external pressure increases the LO and TO phonon frequencies. The pressure-driven RRS effect, according to Eq. (1), causes the intensity of the LO phonon to increase abruptly at first and then to decline smoothly. As the pressure increases, the LO phonon disappears and the sample becomes opaque at 15.7 ± 0.2 GPa, indicating a semiconductor-to-metal phase transition.[9,14–16] This phenomenon is distinct from that revealed by the Raman results of

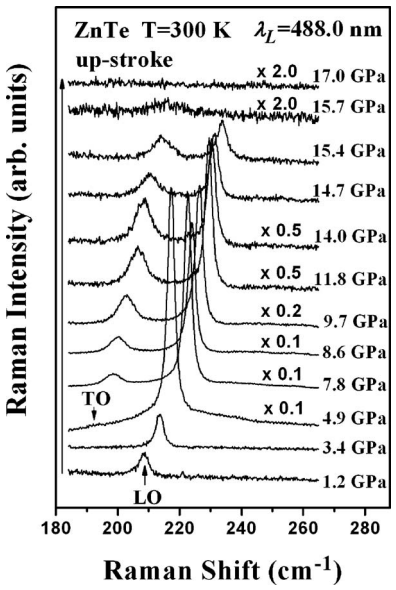

FIG. 3. Up-stroke pressure-dependent Raman spectra of ZnTe at 300 K. Black arrows indicate the LO and the TO phonons. The excitation source is a 488.0 nm line from an Ar^+ laser. The pressure-induced RRS enhancement occurs as the external pressure is increased.

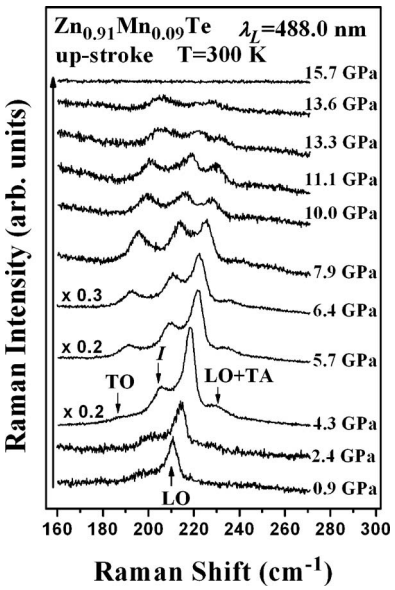

FIG. 4. Up-stroke pressure-dependent Raman spectra of $Zn_{0.91}Mn_{0.09}Te$ at 300 K. LO, TO, LO+TA and impurity (*I*) modes are labeled.

Camacho *et al.*,[12] in which the LO phonon was invisible above 9.6 GPa—far below the critical pressure obtained under the RRS condition discussed herein. The metallic phase transition pressure of ZnTe, measured by the RRS experiment, is consistent with the experimental results of Nelmes *et al.*[13] who determined, using angle-dispersive diffraction techniques with synchrotron radiation source, which crystal structure changed to the ZnTe phase III at 16 GPa. Recently, Shchennikov *et al.*[11] revealed that the sharp drop in resistance from 10^6 to 10^1 Ω in ZnTe at about 13.0–15.0 GPa is related to the transformation into the orthorhombic *Cmcm* phase. The difference between the phase transition pressures obtained by x-ray and electrical resistance methods is attributable to the fact that x-ray techniques determine the phase transition pressure closer to the completion of the transformation, whereas the electrical resistance measurements reveal the beginning of the transition.[11] In Fig. 3, the TO mode does not disappear until at about 17.0 GPa. Other II-VI compounds exhibited a similar phenomenon because transverse surface lattice vibration is allowed in both semiconductor and metal, even though the skin depth (or penetration depth) of the metal for a laser is only several tens of angstroms.[9,14–16] In the down-stroke high-pressure process, only hysteresis is observed and no additional phonon appears.

Figure 4 displays the up-stroke pressure-dependent Raman spectra of $Zn_{0.91}Mn_{0.09}Te$. In addition to the LO and TO modes, a Mn-related impurity mode (*I*) and a double structure associated to LO+TA (transverse acoustic) phonon appear between the LO and TO phonons and at the higher-frequency side of the LO phonon, respectively. As the pressure increases, the impurity mode, the LO phonon, and the TO phonon shift to high frequencies which can be fitted by a quadratic polynomial, as listed in Table I. Since Zn is partially replaced by Mn, the intensity of the Raman spectra is lower than that of ZnTe because the 3*d* orbital of Mn^{2+} ions hybridizes into tetrahedral bonds, causing distortions and altering the overall ZnMnTe crystal symmetry. Furthermore, the LO phonon becomes opaque and disappears at 13.6 ± 0.2 GPa. When the pressure is 15.7 GPa, the TO and *I* modes become invisible. As the Mn content is increased from 0 to 0.09, the semiconductor-to-metal phase transition pressure falls from 15.7 to 13.6 GPa.

Figure 5 plots the phase transition pressure as a function of the Mn content. A decline in the semiconductor-to-metal phase transition pressure (Pt) versus x is shown and is fitted using a quadratic curve, given by $Pt(x)=15.7-25.4x+19.0x^2$ (GPa). As the Mn content increases from 0 to 0.26, the phase transition pressure falls from 15.7 to 10.3 GPa (Table I), indicating that the substituted Mn^{2+} ions tend to reduce the stability of the crystal. The Mn^{2+} ions in $Zn_{1-x}Mn_xTe$ may alter the overall symmetry and soften the lattice by generating large distortions. As the substituted element content increases, the structure becomes less stable. This dependence is similar to other DMS II-VI ternary compounds. Yang *et al.*[15] found that for $Zn_{1-x}Mn_xSe$ compounds, as x is increased from 0.07 to 0.24, the pressure of the metallic phase transition falls from 11.8 to 9.9 GPa. For the $Zn_{1-x}Fe_xSe$ semiconductor, the existence of Fe ions ($x=0.16$) in the ZnSe reduces the semiconductor-metal phase transition pressure from 14.4 to 10.9 GPa.[14] Table I summarizes the pressure-dependent LO, TO, and *I* phonon frequencies derived from quadratic polynomial fits to our measurements. Moreover, the pressure dependence of a mode frequency ω_i can be defined using the dimensionless Grüneisen parameters (γ_i),[19]

$$\gamma_i = -\left(\frac{d \ln \omega_i}{d \ln V}\right) = \frac{1}{\beta}\frac{\partial \ln \omega_i}{\partial p} = \left(\frac{K_0}{\omega_i}\right)\left(\frac{d\omega_i}{dp}\right), \quad (2)$$

where K_0 is the bulk modulus, defined as the reciprocal of the isothermal volume compressibility (β), and V is the molar volume in cm^3/mol. Since the bulk modulus (K_0) of

TABLE I. Pressure-dependent LO, TO, and *I* phonon frequencies (ω_i), $d\omega_i/dp$, calculated mode Grüneisen parameters (γ_i), and phase transition pressures of $Zn_{1-x}Mn_xTe$.

Mn content (x)	Mode	ω_i (cm^{-1})	$d\omega_i/dp$ (cm^{-1}/GPa)	Grüneisen parameter (γ_i)	Phase transition pressure (GPa)
0	LO	$203.6+3.42p-0.10p^2$	$3.42-0.20p$	0.85	15.7 ± 0.2
	TO	$179.2+4.16p-0.11p^2$	$4.16-0.22p$	1.17	
0.09	LO	$206.3+3.34p-0.11p^2$	$3.34-0.22p$	0.82	13.6 ± 0.2
	TO	$177.0+4.26p-0.09p^2$	$4.26-0.18p$	1.22	
	I	$193.4+3.15p-0.08p^2$	$3.15-0.16p$	0.82	
0.14	LO	$207.4+3.29p-0.10p^2$	$3.29-0.20p$	0.80	12.4 ± 0.2
	TO	$176.1+4.30p-0.06p^2$	$4.30-0.12p$	1.24	
	I	$192.0+2.90p-0.06p^2$	$2.90-0.12p$	0.76	
0.22	LO	$208.7+3.15p-0.03p^2$	$3.15-0.06p$	0.76	11.2 ± 0.2
	TO	$175.5+4.43p-0.14p^2$	$4.43-0.28p$	1.27	
	I	$189.7+3.02p-0.05p^2$	$3.02-0.10p$	0.80	
0.26	LO	$209.7+3.06p-0.08p^2$	$3.06-0.16p$	0.74	10.3 ± 0.2
	TO	$174.8+4.55p-0.07p^2$	$4.55-0.14p$	1.31	
	I	$187.4+3.18p-0.08p^2$	$3.18-0.16p$	0.85	

$Zn_{1-x}Mn_xTe$ is unavailable, $K_{0(ZnTe)}=50.5$ GPa is used.[20] As shown in Table I, several conclusions can be drawn. At ambient pressure ($p\sim0$), (i) the LO phonon frequency increases and the TO phonon frequency decreases as the Mn composition increases: the LO-TO splitting increases with Mn content; (ii) $\gamma_{LO}<\gamma_{TO}$ is observed throughout all the specimens, and the ratio γ_{TO}/γ_{LO} rises from 1.38 to 1.77 as the Mn concentration increases from 0 to 0.26. At high pressure, (iii) $d\omega_{LO}/dp<d\omega_{TO}/dp$, such that the LO-TO splitting falls under external pressure for all samples herein; and (iv) $d\omega_I/dp$ and γ_I follow no consistent trend over the entire Mn range of interest ($0.09\leqq x\leqq0.26$). These results demonstrate that under ambient conditions, the manganese ions slightly increase the iconicity of ZnTe. Nevertheless, an externally applied pressure reduces the iconicity and bond length of $Zn_{1-x}Mn_xTe$ crystals.

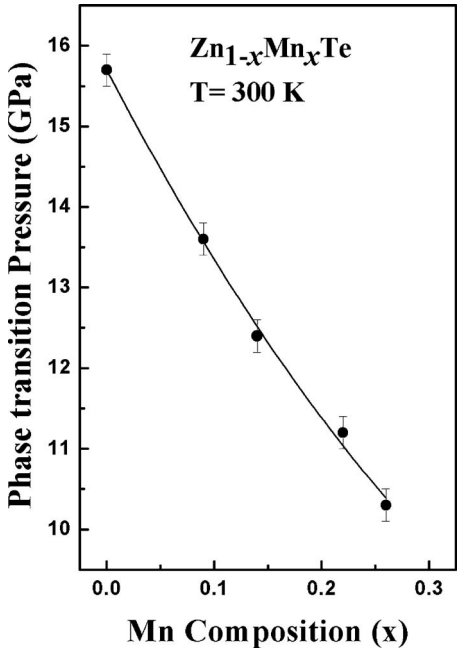

FIG. 5. Mn concentration (x)-dependent semiconductor-to-metal phase transition pressure of $Zn_{1-x}Mn_xTe$. The solid curve is a quadratic polynomial fit, given by $Pt(x)=15.7-25.4x+19.0x^2$ (GPa).

IV. CONCLUSIONS

RRS can enhance the LO and TO phonon intensities in studying pressure-dependent vibrational spectra of $Zn_{1-x}Mn_xTe$ thin films. Intermediate optical phonon mode behavior was identified. The disappearance of the LO phonon, which accompanies a semiconductor-to-metal phase transition in ZnTe, occurs at about 15.7 ± 0.2 GPa. As the Mn content increases from 0 to 0.26, the metallic phase transition pressure falls from 15.7 to 10.3 GPa. Based on the pressure-dependent LO and TO phonon frequencies and Grüneisen parameters (γ_i), externally applying pressure reduces the iconicity of $Zn_{1-x}Mn_xTe$ compound semiconductors.

ACKNOWLEDGMENTS

This work was supported by the Ministry of Education under Grant No. MOE-ATU 97W801-C3 and the National Science Council under Grant No. NSC 96–2112-M-009–026-MY3.

[1]D. L. Peterson, A. Petrou, W. Giriat, A. K. Ramdas, and S. Rodriguez, Phys. Rev. B **33**, 1160 (1986).
[2]M. C. Kuo, J. S. Hsu, J. L. Shen, K. C. Chiu, W. C. Fan, Y. C. Lin, C. H. Chia, W. C. Chou, M. Yasar, R. Mallory, A. Petrou, and H. Luo, Appl. Phys. Lett. **89**, 263111 (2006).
[3]H. Kępa, L. V. Khoi, C. M. Brown, M. Sawicki, J. K. Furdyna, T. M. Giebultowicz, and T. Dietl, Phys. Rev. Lett. **91**, 087205 (2003).
[4]Le Van Khoi, M. Sawicki, K. Dybko, V. Domukhovski, T. Story, T. Dietl, A. Jędrzejczak, J. Kossut, and R. R. Gałązka, Phys. Status Solidi B **229**, 53 (2002).
[5]Le Van Khoi and R. R. Gałązka, Phys. Status Solidi C **3**, 837 (2006).
[6]D. Ferrand, J. Cibert, A. Wasiela, C. Bourgognon, S. Tatarenko, G. Fishman, T. Andrearczyk, J. Jaroszyński, S. Koleśnik, T. Dietl, B. Barbara, and D. Dufeu, Phys. Rev. B **63**, 085201 (2001).
[7]H. Ohno, A. Shen, F. Matsukura, A. Oiwa, A. End, S. Katsumoto, and Y. Iye, Appl. Phys. Lett. **69**, 363 (1996).
[8]H. Munekata, H. Ohno, S. von Molnar, A. Segmüller, L. L. Chang, and L. Esaki, Phys. Rev. Lett. **63**, 1849 (1989).
[9]Y. C. Lin, C. H. Chiu, W. C. Fan, S. L. Yang, D. S. Chuu, M. C. Lee, W. K. Chen, W. H. Chang, and W. C. Chou, J. Appl. Phys. **102**, 123510

(2007).
[10]K. Strössner, S. Ves, C. K. Kim, and M. Cardona, Solid State Commun. **61**, 275 (1987).
[11]V. V. Shchennikov, S. V. Ovsyannikov, A. Y. Derevskov, and V. V. Shchennikov, Jr., J. Phys. Chem. Solids **67**, 2203 (2006).
[12]J. Camacho, I. Loa, A. Cantarero, and K. Syassen, High Press. Res. **22**, 309 (2002).
[13]R. J. Nelmes, M. I. McMahon, N. G. Wright, and D. R. Allan, Phys. Rev. Lett. **73**, 1805 (1994).
[14]C. M. Lin, D. S. Chuu, T. J. Yang, W. C. Chou, J. Xu, and E. Huang, Phys. Rev. B **55**, 13641 (1997).
[15]C. S. Yang, C. S. Ro, W. C. Chou, C. M. Lin, D. S. Chuu, J. Hu, E. Huang, and J. Xu, J. Appl. Phys. **85**, 8092 (1999).
[16]Y. C. Lin, C. H. Chiu, W. C. Fan, S. L. Yang, D. S. Chuu, and W. C. Chou, J. Appl. Phys. **101**, 073507 (2007).
[17]A. Mujica, A. Munoz, and R. J. Needs, Rev. Mod. Phys. **75**, 863 (2003), and references therein.
[18]J. C. Phillips, Phys. Rev. Lett. **27**, 1197 (1971).
[19]M. Blackman and W. B. Daniels, in *Light Scattering in Solids IV*, edited by M. Cardona and G. Güntherodt (Springer, Berlin, 1984), Chap. 8.
[20]A. San-Miguel, A. Polian, M. Gauthier, and J. P. Itié, Phys. Rev. B **48**, 8683 (1993).